

Enhancing the Photoelectric Effect with a Potential-Programmed Molecular Rectifier

Takane Imaoka, Hiroaki Ueda, and Kimihisa Yamamoto*

Chemical Resources Laboratory, Tokyo Institute of Technology, Yokohama 226-8503, Japan

S Supporting Information

ABSTRACT: Dendrimer-based electron rectifiers were applied to photoconducting devices. A remarkable enhancement of the photocurrent response was observed when a zinc porphyrin as the photosensitizer was embedded in the dendritic phenylazomethine (DPA) architecture. The dendrimer-based sensitizer exhibited a 20-fold higher current response than the non-dendritic zinc porphyrin. In sharp contrast, a similar application of the dendrimer with poly(vinylcarbazole) as the electron donor resulted in a decreased response. This is consistent with the idea that the DPA facilitates electron transfer from the core to its periphery along a potential gradient, as predicted by density functional theory calculations.

Molecular interfaces in solid-state materials have a significant effect on the performance of organic thin-layer solar cells, although these devices have mostly been developed by the construction of a “bulk heterojunction”.¹ A remarkable example by Tajima and co-workers demonstrated that the cell performance of conventional P3HT/PCBM devices are drastically improved by the insertion of an intermediate layer with a large dipole moment.² This example suggests that the interfacial design based on an electronic dipole (gradient) has the potential for further improvement. Some previous examples also demonstrated that asymmetrically designed molecules or their aggregates act as a molecular-diode rectifying electron transfer species.³

Implementations of electric heterointerfaces as building blocks in various self-assembling structures would be very important for the design of next-generation materials. We now report that a dendrimer-based system with a potential gradient significantly enhances the photoelectric effect in solid-state materials as a simple photoconducting film, which could be easily prepared by a spin-coating method. In particular, the advantages of using the dendrimer architecture are (1) a unique effect on the electron migration process⁴ on the nano- to mesoscale and (2) a variety of available higher-order hierarchical structures based on the molecular design.⁵ Furthermore, our earlier study focusing on dendrimers demonstrated that specific π -conjugating backbones of dendrimers generate a significant electron density gradient.⁶ One of the other previous applications indicated that they can act as a molecular rectifier during photoinduced electron transfer in dye-sensitized solar cells (DSSCs).⁷ For example, helical architectures were previously proposed to integrate microscopic dipole moments into a large electron polarization

exhibiting a similar asymmetric character in their electronic conductivity.⁸ Alternatively, the dendrimer architecture may also be a candidate for rectification as an added building block.

To estimate the dendrimer effect, we first examined a simple photoconducting film containing a zinc porphyrin as the photosensitizer and a naphthalenediimide derivative (NDI)⁹ as the electron conductor (Figure 1). Dendritic phenylazome-

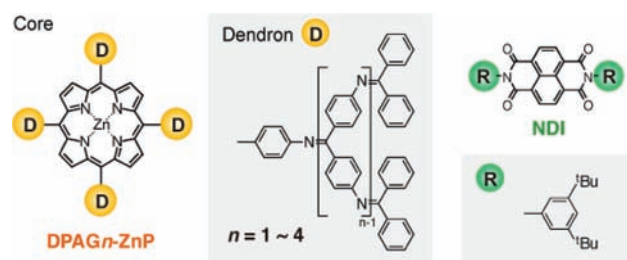


Figure 1. Structures of zinc porphyrin-containing dendrimers (DPAG n -ZnP, $n = 1-4$) used as the sensitizer and the naphthalenediimide derivative (NDI) used as the electron acceptor.

thines (DPAs) with different generation numbers (n) having a zinc porphyrin core (DPAG n -ZnP, $n = 1-4$)¹⁰ together with a nondendritic zinc porphyrin [zinc tetraphenylporphyrin (ZnTPP)] were compared. It should be noticed that the generation number of the dendrimers significantly affects the crystallinity, which could also be related to the carrier generation efficiency. Therefore, we employed a polycarbonate binder (PC) as the host material in which the DPAG n -ZnP dendrimers and NDI electron acceptors were homogeneously dispersed. Chlorobenzene solutions (60 μ L) containing DPAG n -ZnP (1 mmol L⁻¹), NDI (4 mmol L⁻¹), and PC (0.4 mol L⁻¹ for the monomer unit) were spin-coated onto flat indium tin oxide (ITO)/glass electrodes at 2000 rpm. The thicknesses of the dendrimer-containing PC films were determined to be 0.5 μ m. After removal of the organic solvent under vacuum for 12 h, an Al electrode (100 nm thickness) was then vacuum-deposited on each PC film to afford a simple photoconducting cell (Figure 2A). The UV-vis absorption spectra of these cells (Figure 2B) exhibited almost identical absorbance values for the Soret bands (zinc porphyrin core) for each n , suggesting equal molar concentrations of the dendrimers. However, the Soret band of DPAG1-ZnP was quite blue-shifted (425 nm) and broadened relative to those for the other dendrimers (432 nm for $n = 2$, 437 nm for $n = 3$, and

Received: April 4, 2012

Published: May 8, 2012

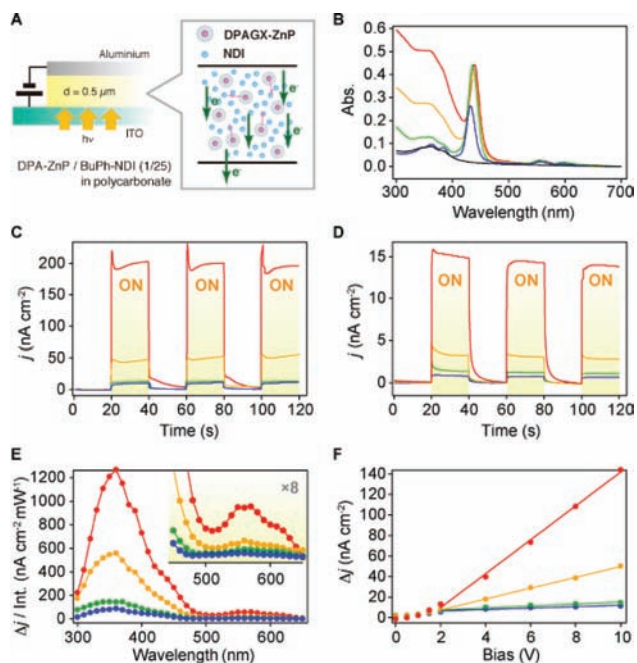


Figure 2. (A) Illustration describing the architecture of the photoconducting cells using DPAGn-ZnP as the sensitizer. (B) UV-vis absorption spectra of the 0.5 μm thick DPAGn-ZnP + NDI + PC composite films. (C, D) Photocurrent density (j) responses as the (C) 438 and (D) 560 nm light was turned on and off with a 10 V applied bias. (E) Action spectra of the photocurrent (Δj) normalized by the illumination energy. (F) Dependence of the photocurrent increment (Δj) on the bias between the two electrodes.

438 nm for $n = 4$), probably as a result of H-aggregation of the zinc porphyrin core. Similarly, NDI, as the electron acceptor (electron-transporting material), was also expected to aggregate vertically to form wires as the electron transport pathways. These wires were indeed observed by transmission electron microscopy (TEM) and atomic force microscopy (AFM) of a sample solvent-cast from a benzene solution of NDI, similar to those found for peryleneimide derivatives (Figure S1).¹¹

The photoconducting properties of these films were examined at an applied bias of 10 V (electric field $2.0 \times 10^5 \text{ V cm}^{-1}$) between the ITO and Al electrodes. Upon repetitive irradiation of the film with monochromatic light (438 or 560 nm) through the ITO electrode, clear photocurrent responses ($\Delta j = j_{\text{ON}} - j_{\text{OFF}}$) were observed (Figure 2C,D). The action spectra of Δj obtained by scanning the excitation wavelength exhibited features similar to the UV-vis absorption spectra, which are mainly composed of the $\pi-\pi^*$ transition of the dendron units (300–400 nm) and the Soret band (ca. 438 nm) and Q bands (550–600 nm) of the porphyrin core (Figure 2E). This means that the carrier generation is triggered by excitation of the dendrimers. The most striking feature of the dependence on the generation number is that a higher generation number produces a higher photocurrent response upon direct excitation of the zinc porphyrin core (Figure 3). As mentioned above, the absorbance values at the λ_{max} corresponding to the Soret and Q bands were almost identical, except for DPAG1-ZnP. In addition, the electron-transporting material NDI was used with the PC binder to retain the intrinsic carrier (electron) mobility in the films for different n . Therefore, the increase in photocurrent with increasing n might be dependent on the carrier formation and recombination steps but not the

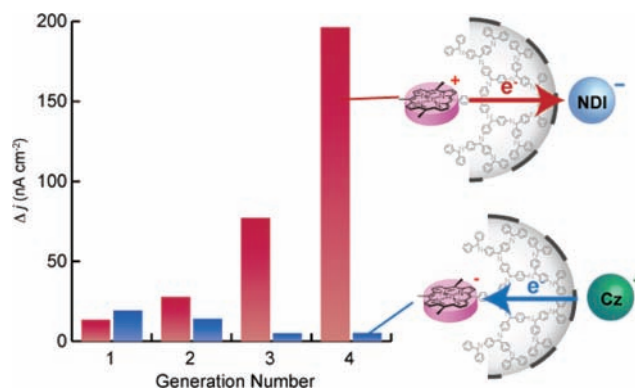


Figure 3. Dependence of the photocurrent on the dendron generation number at an applied bias of 10 V: (red) DPAGn-ZnP + NDI + PC; (blue) DPAGn-ZnP + PVCz.

excitation step. This can be explained as a result of suppressed geminate pair recombination predicted by Onsager theory¹² or less carrier trapping between the encountered free charges.¹³ The dependence of the photocurrents on the applied bias between the two electrodes suggested that the carrier formation efficiency reaches a maximum at 1–2 V. Each sample showed that the increase in the carrier formation started from a bias of ca. 1.0 V (electric field $2.0 \times 10^4 \text{ V cm}^{-1}$) and then exhibited a linear $I-V$ relationship characteristic of ohmic behavior (Figure 2F). This result can be understood by the fact that the efficiency of charge separation in these materials is almost quantitative ($\eta \approx 1$) at these applied electric fields ($>4.0 \times 10^4 \text{ V cm}^{-1}$). The slopes in the ohmic region (2–10 V) were 0.68 (G1), 0.94 (G2), 5.29 (G3) and $16.5 \text{ nA cm}^{-2} \text{ V}^{-1}$ (G4), which may reflect the steady-state carrier mobility regarding the carrier trapping. Especially for DPAG4-ZnP, the host material (PC) was not essential because the dendrimer itself forms an amorphous and homogeneous film by a simple solvent-casting process. Indeed, DPAG4-ZnP and NDI were spin-coated on an ITO electrode without PC to form a homogeneous and transparent film (0.18 absorbance at 441 nm) of which the thickness was ca. 30 nm. In this case, very quick responses were observed upon irradiation at 441 nm (2.7 mW cm^{-2}), and the $j_{\text{ON}}/j_{\text{OFF}}$ ratio was 935 (Figure 4).

This enhancement is considered to be a result of the inherent electronic potential gradient, which provides a large dipole moment of the dendron architecture. To obtain further insight into this gradient, we examined opposite-type photoconducting cells consisting of dendrimers with a zinc porphyrin core (DPAGn-ZnP, $n = 1-4$) and a hole-transporting host material

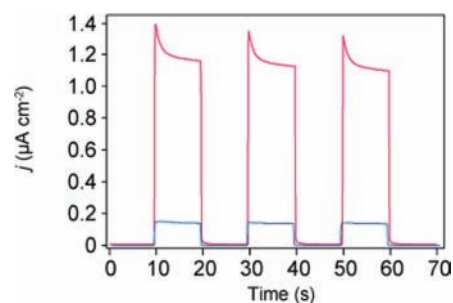


Figure 4. Photocurrent density responses as the light (441 nm) was turned on and off at an applied bias of 1.0 V: (red) DPAG4-ZnP + NDI; (blue) DPAG4-ZnP + PVCz.

such as poly(vinylcarbazole) (PVCz). These cells could be similarly fabricated from chlorobenzene solutions ($60 \mu\text{L}$) containing DPAG n -ZnP (1 mmol L^{-1}) and PVCz (0.4 mol L^{-1} for the monomer unit). The UV-vis absorption spectra also showed that the concentrations of the dendrimers in each film were identical. In sharp contrast to the electron-transporting cells employing NDI, the photocurrents of these hole-transporting cells decreased with increasing generation number (Figure 3). This completely opposite behavior suggests that electron ejection from the core of the dendrimers is facilitated whereas hole ejection (electron injection) is suppressed by a large encapsulation effect of the dendrimer.

To determine the unique intramolecular potential gradient formed in the dendrimers, we performed molecular orbital (MO) calculations on related model compounds. The MO calculations on the phenylazomethine dendrimer DPAG3-Ph and the phenylenevinylene dendrimer DPVG3-Ph at the B3LYP/6-31G* level provided results roughly consistent with the experimental UV-vis absorption and NMR spectra. The Mulliken charge population of each nitrogen atom of DPAG3-Ph showed a higher electron density (negativity) at the inner layer of the dendrimer, suggesting an induction of the electron density gradient (Figure 5). In sharp contrast, we could find no significant difference between the electron densities of the core and peripheral monomers of DPVG3-Ph. This characteristic

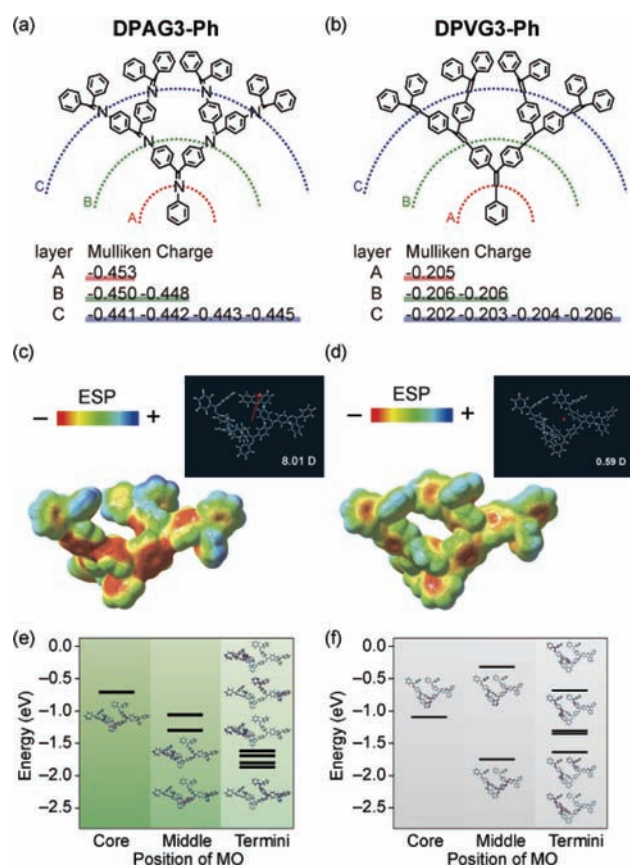


Figure 5. Results of MO calculations (B3LYP/6-31G*) on (a, c, e) DPAG3-Ph and (b, d, f) DPVG3-Ph based on the optimized structures. (a, b) Chemical structures and Mulliken charge populations on the nitrogen atoms or sp^2 carbon atoms in each layer. (c, d) Electrostatic potentials mapped on the electron density isosurfaces. The insets show the dipole moment vectors as red arrows. (e, f) Energies of the unoccupied MOs above the LUMO.

could be observed as molecular dipoles of the dendrimers (Figure 5c,d). The calculated dipole moment of DPAG3-Ph was 8.01 D (Debye), while that of DPVG3-Ph was only 0.59 D. Experimental values of these dipole moments measured by a literature method¹⁴ revealed a significantly higher dipole moment for DPAG3-Ph (5.6 D) than for DPVG3-Ph (2.3 D). This trend was consistent with the molecular calculation results. It is noteworthy that the calculated DPAG3-Ph value was almost equivalent (88%) to the summation of the monomer dipoles ($7 \times 1.3 \text{ D}$). This result suggests a very small contribution of the back-foldings¹⁵ and electron delocalization on the dendrimers, which might compensate for the dipole moment. Furthermore, we found that the lowest unoccupied MO (LUMO) of DPAG3-Ph is mainly distributed on the terminus monomer, whereas the highest occupied MO (HOMO) is on the core-side one. The other unoccupied MOs of DPAG3-Ph above the LUMO displayed potential steps (Figure 5e). However, we could not find any potential steps in the DPVG3-Ph MOs (Figure 5f).

In conclusion, photoinduced carrier generation was enhanced using phenylazomethine dendrimers as a separator between the donor and acceptor materials. Only when the electron donor was incorporated into the dendrimer was the efficiency increased. This result is consistent with the idea that the unidirectional vector of the electron density gradient from the core to the termini facilitates the electron transfer. In a previous approach, modification of the HOMO and LUMO levels (redox potential) of the redox center was the only way to control the electron transfer reactions at the interface. However, the present method allows us to control the apparent redox equilibrium at a specific interface without changing the redox center.

■ ASSOCIATED CONTENT

📄 Supporting Information

Experimental methods, synthesis of the materials, characterization, and TEM and AFM observations of the self-assembling NDI structure. This material is available free of charge via the Internet at <http://pubs.acs.org>.

■ AUTHOR INFORMATION

✉ Corresponding Author

yamamoto@res.titech.ac.jp

Notes

The authors declare no competing financial interest.

■ ACKNOWLEDGMENTS

This work was supported in part by the Core Research for Evolutional Science and Technology (CREST) Program of the Japan Science and Technology Agency (JST) and by a Grant-in-Aid for Scientific Research on Innovative Areas "Coordination Programming" (Area 2107, Grant 21108009) and a Grant-in-Aid for Encouragement of Young Scientists (B) (17750134) from the Japan Society for the Promotion of Science (JSPS).

■ REFERENCES

- (1) (a) Hains, A. W.; Liang, Z.; Woodhouse, M. A.; Gregg, B. A. *Chem. Rev.* **2010**, *110*, 6689. (b) Lee, J. K.; Ma, W. L.; Brabec, C. J.; Yuen, J.; Moon, J. S.; Kim, J. Y.; Lee, K.; Bazan, G. C.; Heeger, A. J. *J. Am. Chem. Soc.* **2008**, *130*, 3619. (c) Thompson, B. C.; Fréchet, J. M. J. *Angew. Chem., Int. Ed.* **2007**, *47*, 58.
- (2) Tada, A.; Geng, Y.; Wei, Q.; Hashimoto, K.; Tajima, K. *Nat. Mater.* **2011**, *10*, 450.

- (3) (a) Díez-Pérez, I.; Hihath, J.; Lee, Y.; Yu, L.; Adamska, L.; Kozhushner, M. A.; Oleynik, I. I.; Tao, N. *Nat. Chem.* **2009**, *1*. (b) Wei, Z.; Kondratenko, M.; Dao, L. H.; Perepichka, D. F. *J. Am. Chem. Soc.* **2006**, *128*, 3134. (c) Zotti, G.; Vercelli, B.; Berlin, A. *Acc. Chem. Res.* **2008**, *41*, 1098.
- (4) (a) Nishimori, Y.; Kanaizuka, K.; Murata, M.; Nishihara, H. *Chem.—Asian J.* **2007**, *2*, 367. (b) Choi, M.-S.; Aida, T.; Luo, H.; Araki, Y.; Ito, O. *Angew. Chem., Int. Ed.* **2003**, *42*, 4060. (c) Li, W.-S.; Kim, K. S.; Jiang, D.-L.; Tanaka, H.; Kawai, T.; Kwon, J. H.; Kim, D.; Aida, T. *J. Am. Chem. Soc.* **2006**, *128*, 10527.
- (5) (a) Astruc, D. *Nat. Chem.* **2012**, *4*, 255. (b) Astruc, D.; Boisselier, E.; Ornelas, C. *Chem. Rev.* **2010**, *110*, 1857. (c) Rosen, B. M.; Wilson, C. J.; Wilson, D. A.; Peterca, M.; Imam, M. R.; Percec, V. *Chem. Rev.* **2009**, *109*, 6275. (d) Tomalia, D. A. *Soft Matter* **2010**, *6*, 456. (e) Percec, V.; Glodde, M.; Bera, T. K.; Miura, Y.; Shiyankovskaya, I.; Singer, K. D.; Balagurusamy, V. S. K.; Heiney, P. A.; Schnell, I.; Rapp, A.; Spiess, H.-W.; Hudson, S. D.; Duan, H. *Nature* **2002**, *419*, 384.
- (6) Albrecht, K.; Yamamoto, K. *J. Am. Chem. Soc.* **2009**, *131*, 2244.
- (7) Satoh, N.; Nakashima, T.; Yamamoto, K. *J. Am. Chem. Soc.* **2005**, *127*, 13030.
- (8) (a) Yasutomi, S.; Morita, T.; Imanishi, Y.; Kimura, S. *Science* **2004**, *304*, 1944. (b) Morita, T.; Kimura, S. *J. Am. Chem. Soc.* **2003**, *125*, 8732.
- (9) Suga, Y.; Arimura, T.; Ide, S.; Sugiwarara, H.; Nishioka, T.; Tachiya, M. *J. Oleo Sci.* **2001**, *50*, 527.
- (10) Imaoka, T.; Tanaka, R.; Arimoto, S.; Sakai, M.; Fujii, M.; Yamamoto, K. *J. Am. Chem. Soc.* **2005**, *127*, 13896.
- (11) (a) Ghosh, S.; Li, X.-Q.; Stepanenko, V.; Würthner, F. *Chem.—Eur. J.* **2008**, *14*, 11343. (b) Sugiyasu, K.; Fujita, N.; Shinkai, S. *Angew. Chem., Int. Ed.* **2004**, *43*, 1229. (c) Zang, L.; Che, Y.; Moore, J. S. *Acc. Chem. Res.* **2008**, *41*, 1596.
- (12) (a) Onsager, L. *Phys. Rev.* **1938**, *54*, 554. (b) Weiss, D. S.; Abkowitz, M. *Chem. Rev.* **2010**, *110*, 479.
- (13) Cohen, Y. S.; Xiao, S.; Steigerwald, M. L.; Nuckolls, C.; Kagan, C. R. *Nano Lett.* **2006**, *6*, 2838.
- (14) Scanu, D.; Yevlampieva, N. P.; Deschenaux, R. *Macromolecules* **2007**, *40*, 1133.
- (15) Ballauff, M.; Likos, C. N. *Angew. Chem., Int. Ed.* **2004**, *43*, 2998.